N89-20083

ESTIMATION OF VELOCITY PERTURBATIONS IN SATELLITE FRAGMENTATION EVENTS

Final Report

NASA/ASEE Summer Faculty Fellowship Program - 1988

Johnson Space Center

Prepared by:	Arjun Tan
Academic Rank:	Associate Professor
University & Department:	Alabama A&M University Department of Physics Normal, Alabama 35762
NASA/JSC	
Directorate:	Space and Life Sciences Directorate
Division:	Solar System Exploration Division
Branch:	Space Science Branch
JSC Colleague:	Gautam D. Badhwar
Date Submitted:	August 12, 1988
Contract Number:	NGT 44-005-803

ABSTRACT

The magnitude, variance and directionality of the velocity perturbations of the fragments of a satellite can shed valuable information regarding the nature and intensity of the fragmentation. Up until now, the only method used to calculate the three orthogonal components of the velocity change consisted of inverting the process of evaluating the changes in the orbital elements of the fragments due to velocity perturbing forces. But the traditional method failed in five different cases: one, when the parent satellite's orbit was circular; two and three, when the true anomaly of the parent was either 0° or 180°; and four and five, when the argument of latitude of the parent was 90° or 270°. This report describes a new method of calculating the velocity perturbations which is free from the shortcomings of the traditional method and could be used in all occasions, provided the fragmentation data and the orbital elements data are consistent with one another.

The method uses the parent satellite's local frame of reference at the time of breakup. The three orthogonal components of the velocity change are derived from three simultaneous equations provided by the changes in specific energy, specific angular momentum and plane angle of the fragment. The fragmentation parameters and the orbital elements of the fragmented satellites are taken from the satellite fragmentation catalog while the orbital elements of the fragments are read from the NORAD and PARCS data files. In order to reverse the decay of the fragment's orbit, the orbital elements of the fragment are propagated backwards to the time of fragmentation.

The velocity perturbations of the fragments of over 20 major satellite fragmentation events were calculated using the new method in this study. This method, together with a recent technique of determining the masses of the fragments, have now furnished a complete set of information about the fragments, including the mass, velocity, momentum, effective cross-sectional area and diameter. The magnitudes and variances of the velcotity perturbations of the fragments of Himawari rocket and Cosmos 839 satellite have reaffirmed their classifications as low intensity explosion and collision induced breakups respectively. The preferred directionality of the fragments of Landsat 3 rocket indicates that the rocket most likely broke up in the "clam" model of low intensity explosion. The residual velocity changes of the fragments of Solwind P-78 satellite provide indications of the general direction of the incoming interceptor. The differential velocity distribution of the fragments of Delta class of breakups could be fitted with a beta function, whereas the cumulative distribution of the same followed a general power law. There is generally a negative correlation between the mass and the velocity change of the fragments. A similar correlation exists between the effective diameter and the velocity change.

INTRODUCTION

To date, nearly one hundred artificial Earth satellites have fragmented in orbit, thus contributing a large proportion of unwanted hazardous material in space (Johnson and Nauer, 1987). To determine retrospectively the cause of fragmentation from the debris characteristics is one of the principal goals of the debris researchers. Over the past few years, we have witnessed significant progress in this area. From the debris data, Culp and McKnight, 1985, developed a satellite fragmentation test to distinguish between explosion and collision induced fragmentation events. Based on the distribution of plane change angle and radar cross-sections of known fragmentation events, Badhwar, et al., 1988, devised a scheme to distinguish between the three classes of satellite breakups: low intensity explosion induced, high intensity explosion induced and hypervelocity collision induced breakups. Furthermore, a technique now exists to determine the masses of the fragments of a satellite from the history of their orbital elements and radar cross-sections (Badhwar and Anz-Meador, 1988).

One of the most important quantities in satellite fragmentation events is the velocity change suffered by a fragment during the breakup. For instance, the magnitudes of these velocity changes may be used as indications as to whether a fragmentation is due to low intensity explosion, high intensity explosion or hypervelocity impact, based on the study of Bess, 1975. Also, the directionality of the velocity perturbations may give clues as to the nature and intensity of the explosion as per the analysis of Benz, et al., 1987. However, up until now, no satisfactory method existed to calculate all three components of the velocity change. The traditional method consisted of inverting the process of evaluating the changes of the orbital elements due to velocity perturbing forces from Meirovitch, 1970, and had been used by McKnight, 1986; Kling, 1986; and Tan, 1987. But Tan, 1987, showed that the calculated radial component of the velocity change became exceedingly large when the parent satellite's orbit was nearly circular or when the fragmentation took place near the apsidal points. Similarly, the calculated cross-range component of the velocity change became singularly high when the argument of latitude was 90° or 270°.

In order to obtain a method which is free from the singularities of the traditional method and which could be used in all occasions, Reynolds, 1987, initiated a new approach of estimating the velocity changes. This approach parallels an earlier study by Wiesel, 1978, and was refined by Badhwar, NASA scientist; Tan, summer fellow; and Reynolds, Lockheed scientist at NASA-JSC this summer. The method is now fully operational and coupled with the technique of Badhwar and Anz-Meador, 1988, can furnish a complete set of information about the fragments, including the mass, velocity, momentum, effective cross-sectional area and diameter. A brief description of the method is contained in this report. The report also summarizes the results obtained by analyzing the velocity perturbations in the major breakup events calculated by this method.

METHOD

In order to calculate the velocity perturbations imparted to the fragments, it is convenient to use the parent satellite's local frame of reference at the point of breakup (Wiesel, 1978; Reynolds, 1987). The three orthogonal directions are then defined by the radial and the down-range directions in the plane of the orbit and the cross-range direction perpendicular to the plane of the orbit and along the angular momentum vector (Fig.1). In this coordinate system, the velocity $\vec{v}$ of the parent has the components v_r, v_d and 0. From elementary astrodynamics, we have

$$v = [\mu(\frac{2}{r} - \frac{1}{a})]^{\frac{1}{2}} , \tag{1}$$

$$v_d = \frac{1}{r} [\mu a(1-e^2)]^{\frac{1}{2}} , \tag{2}$$

and $$v_r = \pm (v^2-v_d^2)^{\frac{1}{2}} , \tag{3}$$

where a is the semi major axis and e the eccentricity of the parent's prbit, r is the radial distance to the breakup point and μ is the gravitational parameter. In Eq.(3), the plus sign corresponds to the ascending mode of the satellite (true anomaly $\nu < 180°$) whereas the minus sign corresponds to descending mode ($\nu > 180°$).

Upon fragmentation, the velocity of a fragment $\vec{v}'$ will have the components v_r+dv_r, v_d+dv_d and dv_x, where dv_r, dv_d and dv_x are the velocity perturbations received by the fragment during the breakup. In consequence, the fragment would suffer changes in energy, angular momentum and orbital inclination. The change in specific energy is given by

$$E'-E = \tfrac{1}{2}(v'^2-v^2) = - \frac{\mu}{2} (\frac{1}{a'} - \frac{1}{a}) ,$$

or, $$\tfrac{1}{2}[(v_r+dv_r)^2 + (v_d+dv_d)^2 + dv_x^2 - v_r^2 - v_d^2] = - \frac{\mu}{2} (\frac{1}{a'} - \frac{1}{a}) , \tag{4}$$

where a' is the semi major axis of the fragment's orbit. Similarly, if e' is the eccentricity of the fragment's orbit, the change in specific angular momentum is given by

$$h'^2-h^2 = |\vec{r} \times \vec{v}'|^2 - |\vec{r} \times \vec{v}|^2 = \mu a'(1-e'^2) - \mu a(1-e^2) ,$$

or, $$r^2[(v_d+dv_d)^2 + dv_x^2 - v_d^2] = \mu a'(1-e'^2) - \mu a(1-e^2) . \tag{5}$$

Finally, the plane change angle θ of the perturbed orbit from the unperturbed is given by (vide Fig.2)

$$\tan \theta = \frac{dv_x}{v_d+dv_d} . \tag{6}$$

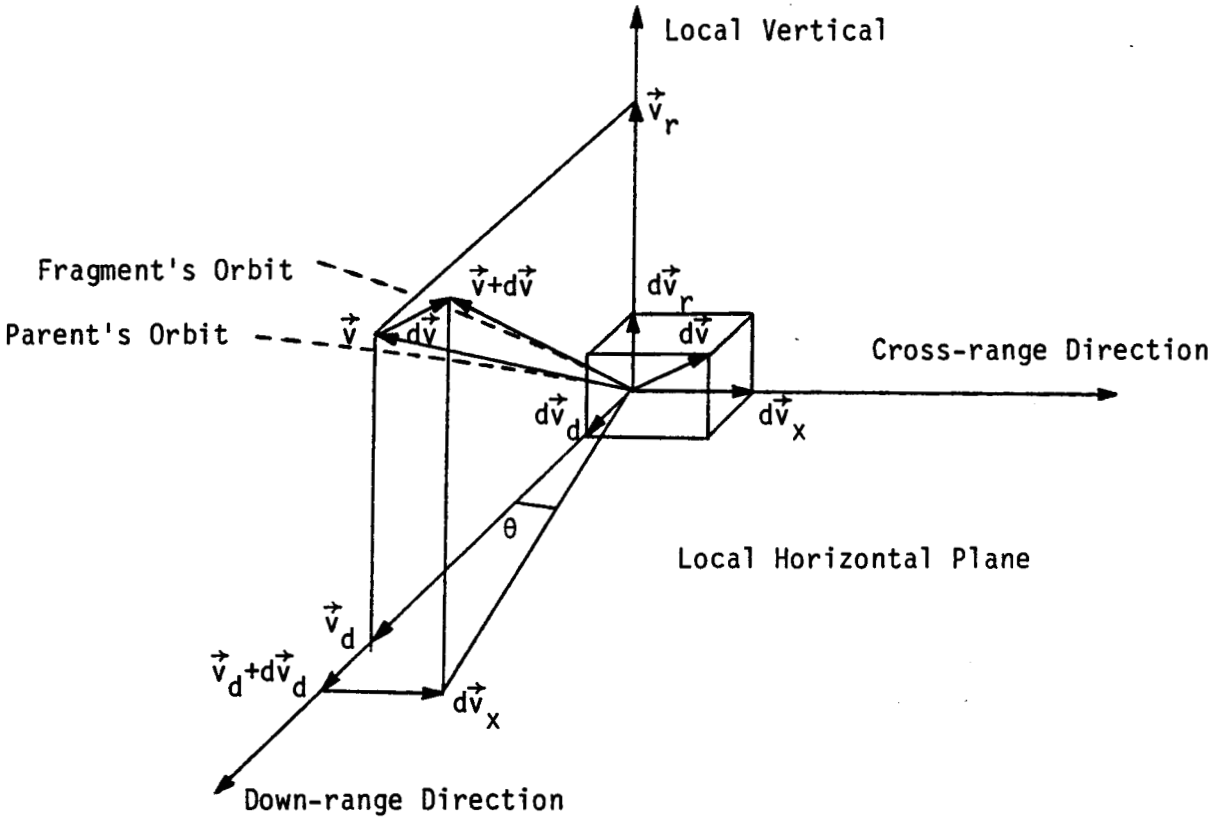

Fig.1. The parent satellite's local coordinate system and the velocity components of the parent and the fragment.

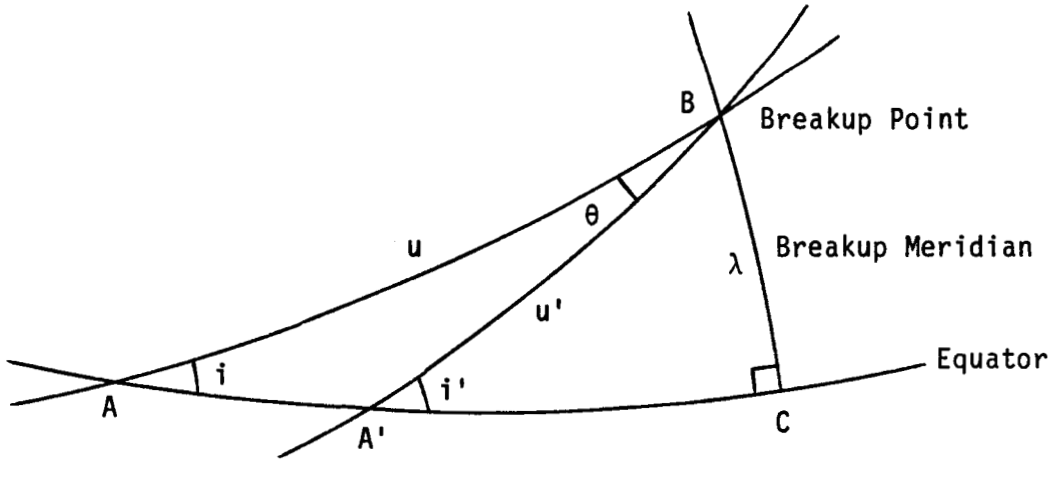

Fig.2. Breakup (spherical) triangles for the parent and the fragment.

Equations (4), (5) and (6) comprise three simultaneous equations from which the three unknowns dv_r, dv_d and dv_x can be solved in principle. After some manipulations and elimination, we arrive at the expressions for the velocity perturbations

$$dv_r = \pm \left[\mu\left(\frac{2}{r} - \frac{1}{a'}\right) - \frac{\mu}{r^2}\, a'(1-e'^2)\right]^{\frac{1}{2}} - v_r \ , \tag{7}$$

$$dv_d = \frac{\cos\theta}{r}\left[\mu a'(1-e'^2)\right]^{\frac{1}{2}} - v_d \ , \tag{8}$$

and $$dv_x = \frac{\sin\theta}{r}\left[\mu a'(1-e'^2)\right]^{\frac{1}{2}} \ . \tag{9}$$

In Eq.(7), the plus sign corresponds to the ascending mode of the fragment (true anomaly $\nu' < 180°$), whereas the minus sign corresponds to descending mode ($\nu' > 180°$). Elsewhere, the dominance of v_d over dv_d ensures the retention of only the positive sign of the square root in Eqs.(8) and (9). Equations (7), (8) and (9) can be shown to be equivalent to Reynolds' (1987) equations, which are expressed in normalized quantities.

The plane change angle θ can be expressed as a function of the inclinations i and i' of the parent's and the fragment's orbits respectively and λ, the latitude of the breakup point (cf. Badhwar, et al., 1988). Applying both the cosine laws to the spherical triangle AA'B of Fig.2 and the sine law to the triangles ABC and A'BC and substituting, we get

$$\theta = \pm \cos^{-1} \frac{\cos i \cos i' + (\cos^2\lambda - \cos^2 i)^{\frac{1}{2}}(\cos^2\lambda - \cos^2 i')^{\frac{1}{2}}}{\cos^2\lambda} \ . \tag{10}$$

Here, the plus sign corresponds to $i' > i$ and the minus sign corresponds to $i' < i$.

The true anomaly ν' of the fragment at the time of breakup, which dictates the sign of $v_r + dv_r$ in Eq.(7) is determined from the argument of latitude u' and the argument of perigee ω' of the fragment at the time of breakup as follows.

$$\nu' = u' - \omega' \ . \tag{11}$$

Applying the sine law to the spherical triangle A'BC of Fig.2, we get

$$u' = \sin^{-1}\left(\frac{\sin\lambda}{\sin i'}\right) \quad \text{or} \quad 180° - \sin^{-1}\left(\frac{\sin\lambda}{\sin i'}\right) \ , \tag{12}$$

where the first solution corresponds to northbound motion of the fragment and the second corresponds to southbound motion at the time of fragmentation. Since the argument of perigee is perturbed by the oblateness of the earth, the argument of perigee of the fragment at the time of observation ω'_o is different from that at the time of fragmentation ω'. From the rate of precession derived by King-Hele, 1964, we get

$$\omega' = \omega'_o - \frac{4.98(5\cos^2 i' - 1)\Delta t}{(a'/r_o)^{7/2}(1-e'^2)^2}, \tag{13}$$

where Δt is the time of observation from the time of fragmentation. Here, ω', ω'_o are expressed in degrees and Δt is expressed in days. It was verified from the successive NORAD data that the true anomaly predicted this way was generally accurate to within 2 degrees per year of the observed value, thus demonstrating the validity of this technique.

The fragmentation parameters and the orbital elements of the fragmented satellites are taken from the fragmentation catalog by Johnson and Nauer, 1987, while the orbital elements of the fragments are read from the NORAD data files. The apogee and perigee heights are normally converted into the semi major axis and eccentricity. Thus

$$a = \frac{2r_o + h_a + h_p}{2}, \tag{14}$$

$$e = \frac{h_a - h_p}{2r_o + h_a + h_p}, \tag{15}$$

$$r = r_o + h, \tag{16}$$

$$a' = \frac{2r_o + h'_a + h'_p}{2}, \tag{17}$$

and

$$e' = \frac{h'_a - h'_p}{2r_o + h'_a + h'_p}, \tag{18}$$

where r_o is the reference radius of the earth, h_a and h_p are the apogee and perigee heights of the parent, and h'_a and h'_p are those of the fragment.

Atmospheric drag causes decay in satellite orbits, particularly at low altitudes, making both the semi major axis and eccentricity smaller. This introduces substantial errors in the velocity perturbations calculations when the debris data were measured long after the fragmentation event, which is quite often the case. In order to compensate for this error, the debris parameters are propagated backwards to the time of fragmentation by running the orbital decay code of Mueller, 1981 in reverse. For this purpose, the area-to-mass ratio of the fragments are first determined by the technique of Badhwar and Anz-Meador, 1988. The solar flux in that period, which determines the atmospheric densities, is read from the NOAA data base.

RESULTS

In this study, over 20 major satellite fragmentation events were studied, each of which produced at least 40 cataloged objects. The fragmentation parameters and the orbital elements of the parent satellite were taken from the satellite fragmentation catalog by Johnson and Nauer, 1987 and the orbital elements of the fragments were read from the NORAD data files. In addition, the PARCS data for the Solwind P-78 fragments were used.

Figure 3 shows the frequency distributions of the velocity perturbations of the fragments of Himawari rocket body and Cosmos 839 satellite. The frgmentation of the Himawari rocket belongs to the Delta class of fragmentation due to low intensity explosion, whereas Cosmos 839 was believed to have been an ASAT target which was destroyed through collision (cf. Johnson and Nauer, 1987). The magnitudes of the velocity changes are much smaller in the latter case as compared with the former, which lend support to the classifications based on the study of Bess, 1975. Further, the velocity changes in the Cosmos 839 fragmentation event have a much smaller variance compared with those of the Himawari explosion, which are again consistent with the classifications (vide Badhwar and Tan, 1988).

Figure 4 depicts the two- and three-dimensional plots of the velocity perturbations of the fragments of Solwind P-78 satellite which was intentionally destroyed through hypervelocity impact (Kling, 1986). The velocity perturbations show considerable scatter and their magnitudes are significantly larger than those in the alledged Soviet ASAT collisions. Conspicous in the figures are three fragments with large velocity changes in all three directions.

In order to study the directionality of the fragments, we define two angles as follows: the colatitude $\theta = \cos^{-1}(dv_r/dv)$, $0° < \theta < 180°$; and the longitude $\phi = \tan^{-1}(dv_x/dv_d) + n\ 180°$, $-180° < \phi < 180°$, where $n = 0$ for $dv_d > 0$, $n = 1$ for $dv_d < 0$, $dv_x > 0$, and $n = -1$ for $dv_d < 0$, $dv_x < 0$. Note that the colatitude is not the plane change angle defined earlier. The angles for each fragment of a breakup event are calculated and then plotted. Fig.5a is an angular plot of the fragments of Landsat 3 rocket as in a Mercator projection of the world map. The preferred direction in which most fragments emerged clearly shows that the distribution of fragments was highly anisotropic in this case. Based on the analysis of Benz, et al., 1987, we infer that Landsat 3 was most likely broken in the "clam" model of low intensity explosion. Fig.5b is a similar plot with the velocity changes in addition. Since the Mercator plots are area-distorted with the polar fragments appearing less dense compared with the equatorial, we have calculated the fragment flux per unit solid angle, where the elementary solid angle is $d\Omega = \sin\theta\ d\theta\ d\phi$. Fig.5c exhibits the fragment flux per unit solid angle, which is now free from area distortion.

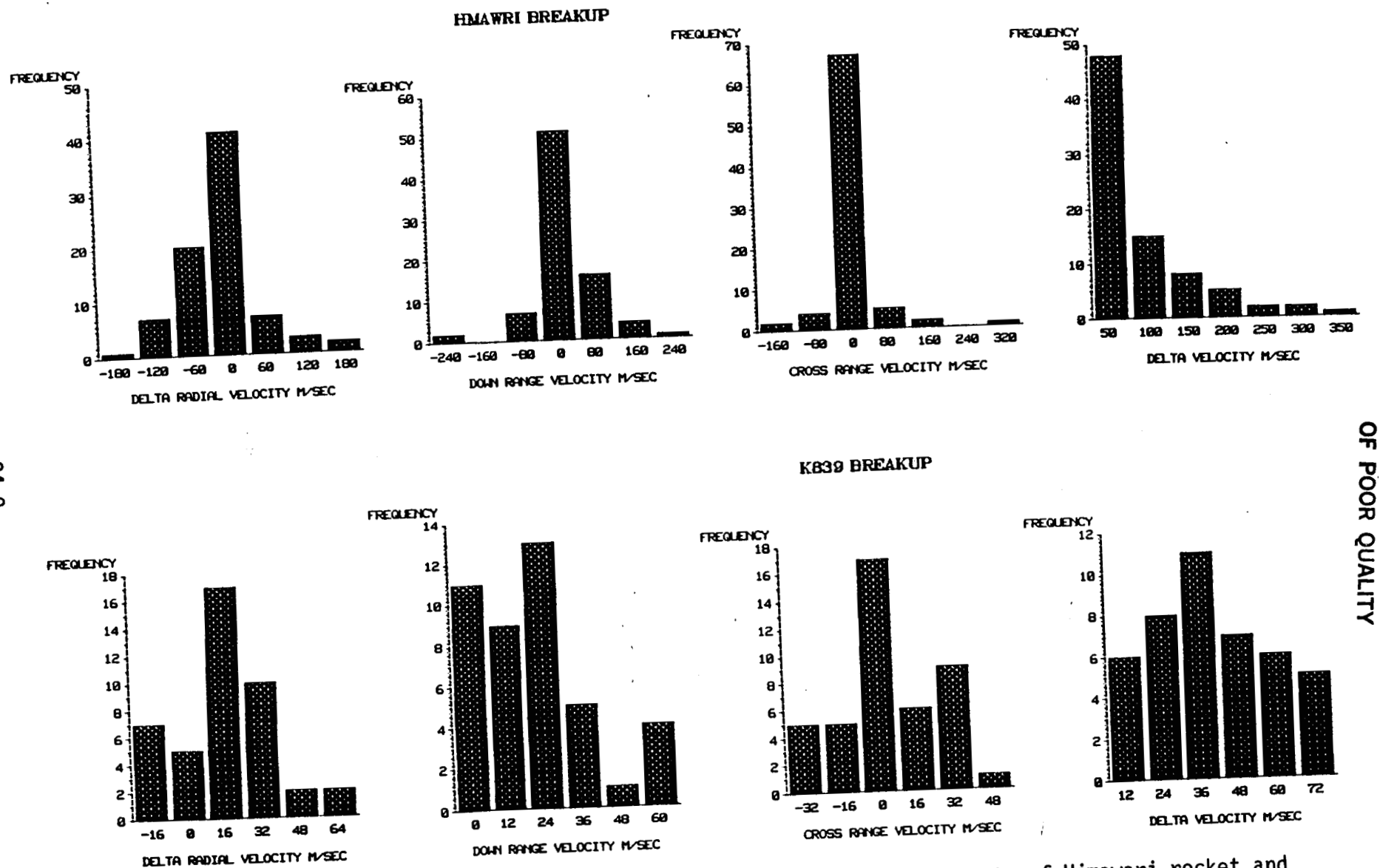

Fig.3. Frequency distributions of the velocity perturbations of the fragments of Himawari rocket and Cosmos 839 satellite.

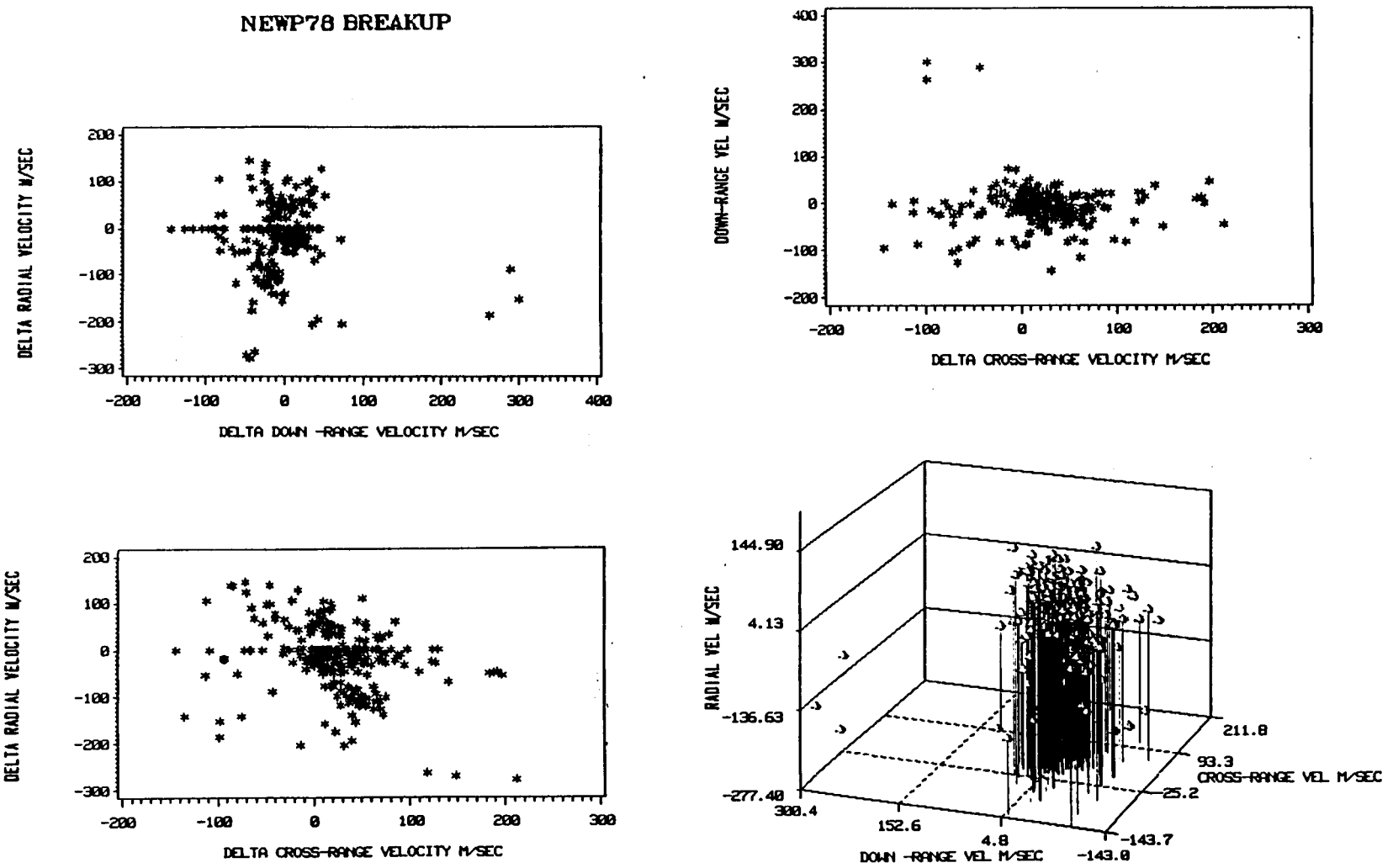

Fig.4. Two- and three-dimensional plots of the velocity perturbations of the fragments of Solwind P-78 satellite.

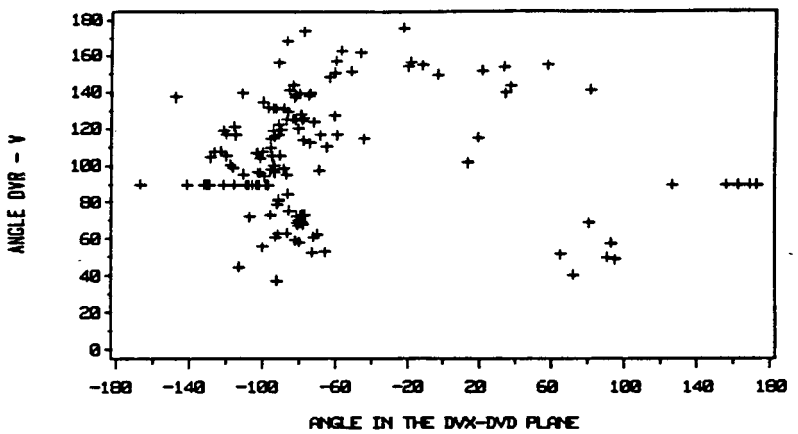

Fig.5a. Angular distribution of fragments of Landsat 3 rocket.

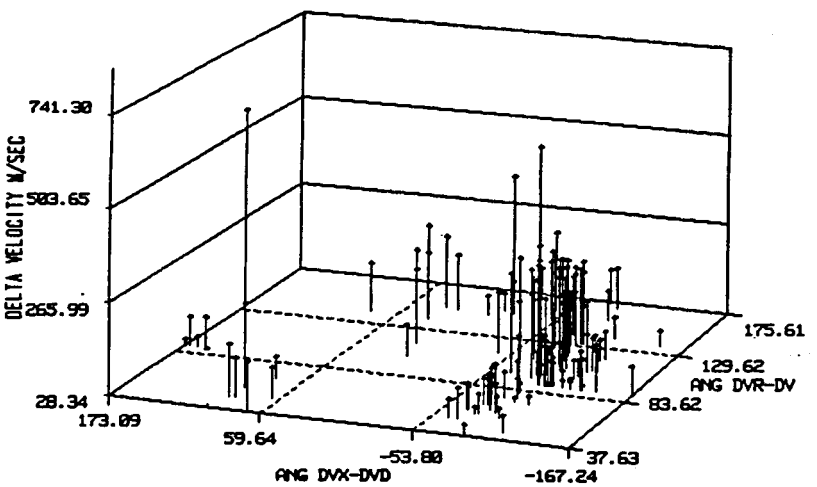

Fig.5b. Angular plot of fragments of Landsat 3 with velocity change.

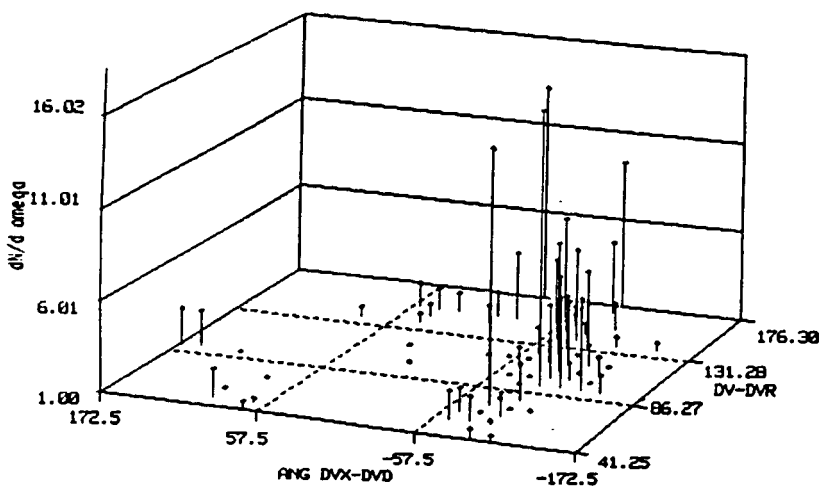

Fig.5c. Distribution of fragment flux per unit solid angle.

Analysis of the Solwind P-78 fragmentation event with the PARCS data taken immediately after the fragmentation shows that the mean velocity changes of all fragments, i.e., the mean dv_r, dv_d and dv_x do not add up to zero but were -17.6, -4.9 and 22.5 meter per second respectively. For the lack of orbital element history, the masses of the fragments could not be determined. However, assuming equal masses for all fragments, we find a net transfer of momentum in the direction of $\theta = 103°.1$ and $\phi = 102°.3$, which could imply that the interceptor most probably arrived from the general direction of $\theta = 76°.9$ and $\phi = -77°.7$ in the local frame of reference of Solwind P-78.

Figure 6a shows the differential distribution of the fragments of all Delta rocket breakups (NOAA, Landsat and Himawari) versus velocity change. The curve, which shows considerable extension in velocity, can be fitted with a beta function of the form

$$\frac{dN}{d(dv)} = A\ (dv/dv_{max})^{\alpha-1}\ (1 - dv/dv_{max})^{\beta-1}\ . \qquad (19)$$

Fig.6b is a plot of the cumulative number of fragments of the above category of breakups with velocity change greater than dv versus the velocity change. The cumulative distribution gives a smoother curve which is given by a power law of the form

$$N(>dv) = A\ (dv + B)^{-C}\ . \qquad (20)$$

The constants α, β, A, B, C etc. which determine the shapes of the distributions, could be used as characteristic parameters of an individual or a class of breakup events.

The correlation, if any, between the masses and the velocity changes of the fragments could be found once the masses of the fragments are determined by the technique of Badhwar and Anz-Meador, 1988. Fig.7 is a plot of mass against the velocity change of the fragments of the Spot-1 Viking rocket. Amidst considerable scatter, the trend for a negative correlation is clearly noticeable.

The change in momentum suffered by a fragment during the breakup can be computed from the masses and the velocity changes thus determined. Fig.8 is an example of the cumulative distribution of the fragments of NOAA 5 rocket versus momentum change. The data points were fitted with an expression similar to Eq.(20).

The effective diameter of the Delta class of fragmentations have been computed from the effective cross-sectional area and plotted against the velocity change with error bars in Fig.9. Finally, the distribution of the fragments of the same class of events are plotted against the velocity change and effective diameter in Fig.10. A pyramid-shaped distribution with unequal slopes on the opposite sides is clearly visible. This distribution can be used in the study of the evolution of debris cloud after a model low intensity explosion.

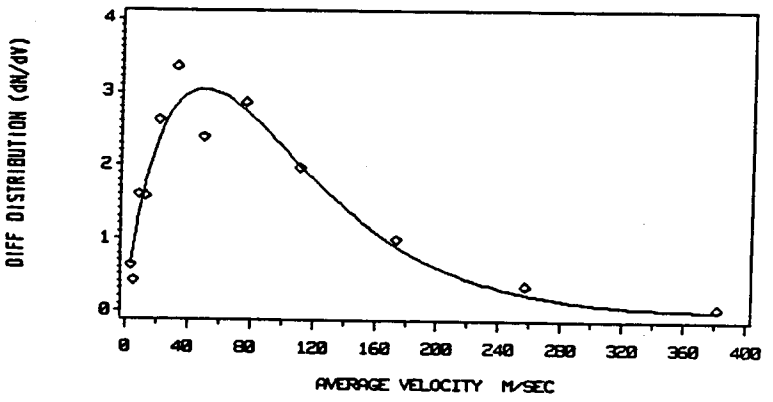

Fig.6a. Differential distribution of fragments of Delta class fragmentations vs. velocity change.

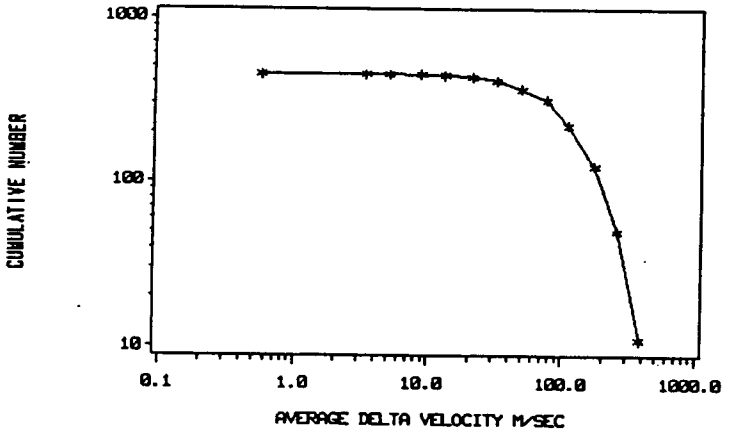

Fig.6b. Cumulative distribution of fragments of Delta class fragmentations vs. velocity change.

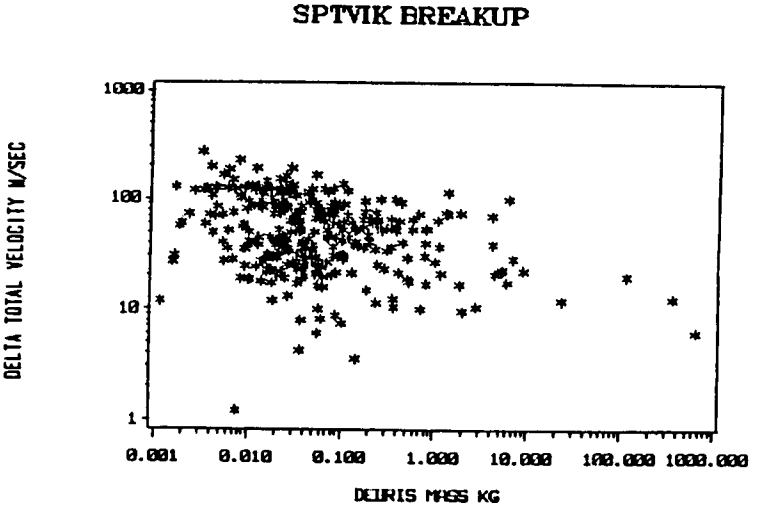

Fig.7. Velocity change of fragments of Spot-1 Viking rocket vs. fragment mass.

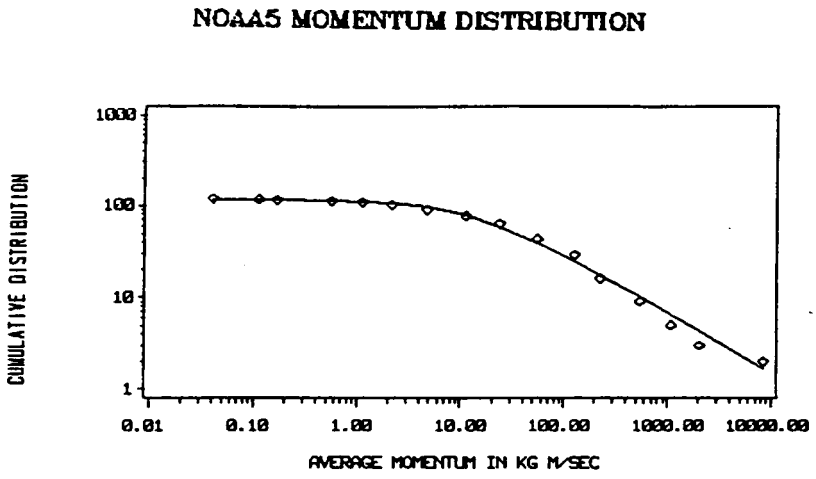

Fig.8. Cumulative distribution of fragments of NOAA 5 rocket vs. average momentum change.

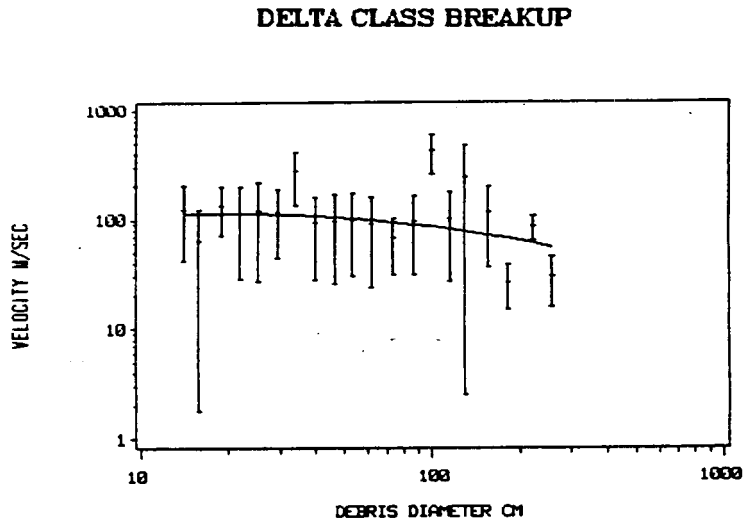

Fig.9. Velocity perturbations of fragments of Delta class fragmentations vs. effective fragment diameter.

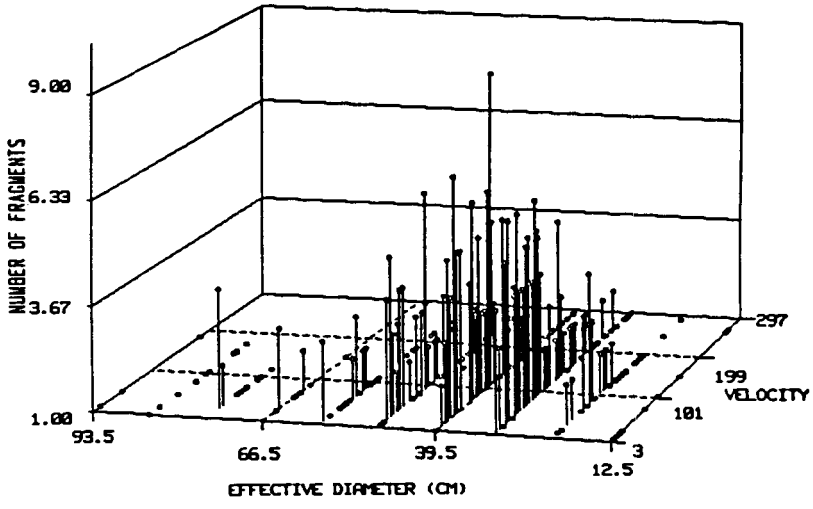

Fig.10. Distribution of fragments of Delta class fragmentations with velocity change and effective fragment diameter.

REFERENCES

Badhwar, G. D.; and Anz-Meador, P. D.: Determination of the area and mass distribution of orbital debris fragments, preprint, 1988.

Badhwar, G. D.; and Tan, A.: Analysis and interpretation of satellite fragmentation data, J. Ala. Acad. Sci., Vol. 59, 1988, p. 153.

Badhwar, G. D.; Potter, A. E.; Anz-Meador, P. D.; and Reynolds, R. C.: Characteristics of satellite breakups from radar cross-section and plane change angle, J. Spacecraft and Rockets, Vol. 44, July 1988.

Benz, F. J.; Kays, R. L.; Bishop, C. V.; and Eck, M. B.: Explosive fragmentation of orbiting propellant tanks, unpublished, 1987.

Bess, T. D.: Mass distribution of orbiting man-made space debris. NASA TN D-8108, 1975.

Culp, R. D.; and McKnight, D. S.: Distinguishing between collision-induced and explosion-induced satellite breakup through debris analysis. Paper presented at AAS/AIAA Astrodynamics Specialist conference, Vail, Colorado, 1985.

Johnson, N. L.; and Nauer, D. J.: History of on-orbit satellite fragmentations, Teledyne Brown Engg. Report CS88-LKD-001, 1987.

King-Hele, D.: Theory of satellite orbits in an atmosphere, Butterworths, 1964, p. 4.

Kling, R.: Postmortem of a hypervelocity impact, Teledyne Brown Engg. Report CS86-LKD-001, 1986.

McKnight. D. S.: Discerning the cause of satellite breakups. Paper presented at the 62nd Annual AAS meeting, Boulder, Colorado, 1986.

Meirovitch, L.: Methods of Analytical Dynamics, McGraw-Hill, 1970, pp. 453-456.

Mueller, A. C.: The decay of low earth satellite, Lockheed Engg. Report 17520, 1981.

Reynolds, R. C.: Evolution of the debris cloud immediately after a satellite breakup in orbit, unpublished, 1987.

Tan, A.: Analysis and interpretation of satellite fragmentation data in NASA CR 172009, W. B. Jones and S. H. Goldstein ed., 1987.

Wiesel, W.: Fragmentation of asteroids and artificial satellites in orbit, Icarus, Vol. 34, 1978, pp. 99-116.